

## Machine-detector interface studies for a multi-TeV muon collider

---

**Daniele Calzolari<sup>1,\*</sup> and Kyriacos Skoufaris<sup>1</sup>**

*CERN, Espl. des Particules 1, 1211 Meyrin, Switzerland*

*E-mail: [daniele.calzolari@cern.ch](mailto:daniele.calzolari@cern.ch)*

Circular muon colliders offer the prospect of colliding lepton beams at unprecedented center-of-mass energies. The continuous decay of stored muons poses, however, a significant technological challenge for the collider and detector design. The secondary radiation fields induced by decay electrons and positrons can strongly impede the detector performance and can limit the lifetime of detector components. Muon colliders therefore require an elaborate interaction region design, which integrates a custom detector shielding together with the detector envelope and the final focus system. In this paper, we present design studies for the machine-detector interface and we quantify the resulting beam-induced background for different center-of-mass energies. Starting from the optics and shielding design developed by the MAP collaboration for 1.5 TeV, we devise an initial interaction region layout for the 10 TeV collider. In particular, we explore the impact of lattice and shielding design choices on the distribution of secondary particles entering the detector. The obtained results serve as crucial input for detector performance and radiation damage studies.

*41st International Conference on High Energy physics - ICHEP2022  
6-13 July, 2022  
Bologna, Italy*

---

<sup>1</sup>For the International Muon Collider Collaboration.

\*Speaker

## 1. Introduction

Circular muon colliders (MC) are considered a promising option as future precision and discovery machines in high-energy physics. Being much less limited by synchrotron radiation emission than electrons and positrons, circular muon colliders offer the prospect of significantly higher collision energies than electrons-positrons colliders. Furthermore, the collision of elementary particles allows for a full exploitation of the center-of-mass energy for short-distance reactions, while in hadron colliders the energy is shared among constituents of the colliding particles [1]. Despite the advantages, the design of a muon collider involves a large number of technical and radiation challenges and has been less explored and studied than the other options [2]. Recently, a renewed effort and interest has grown toward the muon collider. This culminated in the formation of the International Muon Collider Collaboration (IMCC) [3], which aims in studying the main design requirements for a collider with  $\sqrt{s}=10+$  TeV, with a possible pre-stage at  $\sqrt{s}=3$  TeV.

Even at energies as high as a few TeV, muons still have a relatively short lifetime (0.1 s in a 10 TeV collider, against  $2.2 \mu\text{s}$  in the rest frame), decaying into neutrinos and a positron or electron. Neutrinos carry away around 2/3 of the muon energy, while the rest is retained by the electrons/positrons. The latter are responsible for most of the head load and radiation damage in the accelerator. When the decay occurs in the proximity of the interaction point (IP), the resulting radiation fields can impede the detector performance, representing the main source of the so-called beam induced background (BIB).

This study addresses a key component of the muon collider, the machine-detector interface (MDI). MDI design studies for muon colliders have been performed previously in the context of the US Muon Accelerator Program (MAP) [4]. The considered center-of-mass energies ranged from 126 GeV [5] to exploit the muon collider as a Higgs factory, up to 1.5 TeV [6] and 3 TeV [7]. More recently, the BIB in 1.5 TeV and 3 TeV machines has been reassessed within a new simulation framework, showing a good agreement with past simulations [8]. In this paper, we present first MDI studies for a higher-energy collider, with a center-of-mass energy of  $\sqrt{s}=10$  TeV. The studies are based on the FLUKA Monte Carlo code [9, 10]. The scope of the paper is to provide an assessment of the background particle flux into the detector. The results will serve as input for detector performance and radiation damage studies.

## 2. Decay-induced background in a 10 TeV muon collider

Assuming a design luminosity at  $\sqrt{s}=10$  TeV of  $2 \times 10^{35} \text{ cm}^{-2} \text{ s}^{-1}$ , the beams need to be strongly focused in the interaction point (IP), where the  $\beta$ -function is squeezed to  $\beta^* = 1.5$  mm. With a maximum field of 20 T at the inner bore of the quadrupoles, assuming a distance  $L^*$  of 6 m between the IP and the first magnet, a  $\sim 30$  m-long final focus triplet is required. To facilitate the aperture and field requirements, the innermost focusing quadrupole has been split into three parts. The section downstream of the triplet contains the chromaticity correction scheme, consisting of combined-function quadrupoles and sextupoles. The adopted layout is shown in Figure 1. In the detector region ( $2 \times L^*$ ), a 5 T solenoidal field is present.

To reduce the decay-induced background, conical shielding elements need to be integrated in the interaction region in close proximity to the IP [11]. These so-called nozzles extend until the first

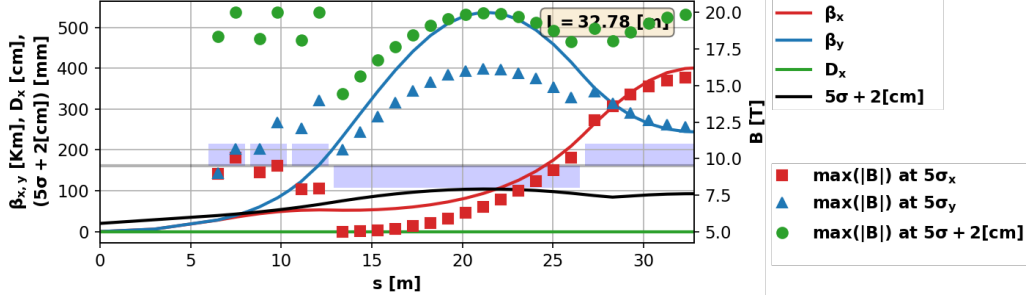


**Figure 1:** Lattice for the final focus and the chromaticity correction region of the  $\sqrt{s}$  10 TeV muon collider.

magnet ( $L^* = 6$  m) and must be made of a high- $Z$  material as tungsten to shield the electromagnetic cascades. On the outer side of the nozzle, a layer of borated polyethylene or a similar material is needed to reduce the neutron flux into the detector. The nozzle design has been carefully optimized for energies up to 1.5 TeV in the scope of the MAP studies [11], and it is considered as the baseline for the new 1.5 TeV studies [8], as well as for the 10 TeV studies presented in this paper.

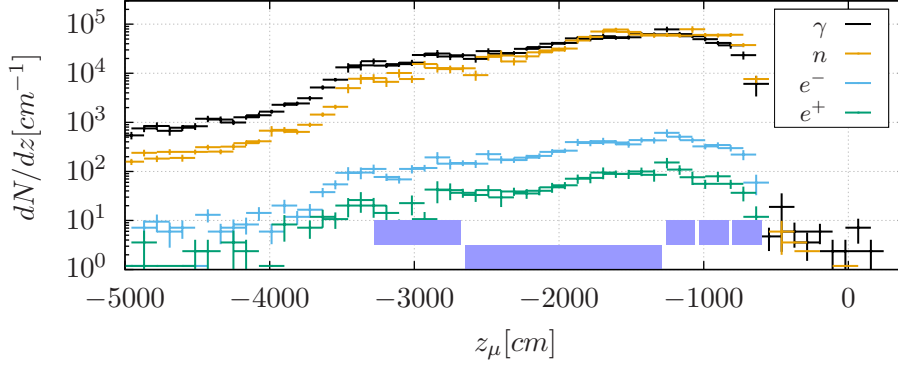
In the present work, the muon position and direction during the decay are sampled from a matched beam phase-space distribution. The chosen particle production and transport cuts in the Monte Carlo simulation are the same as in past works [8, 11]. Neutrons are simulated down to thermal energy, while other particles are discarded below 100 keV. For simplicity, we simulate only one of the two single-bunch beams, assuming a bunch intensity of  $2 \times 10^{12} \mu$ . Whereas, to reach the target luminosity, even  $1.8 \times 10^{12} \mu$  are sufficient. Muon decays are sampled up to a distance of 200 m from the IP.

Table 1 shows the number of secondary particles entering the detector envelope through the shielding or the central vacuum chamber, assuming a MAP-like nozzle. The table compares the present 10 TeV results to the 1.5 TeV simulations reported in Ref. [8]. Only the most abundant particle species are shown. The overwhelming contribution in terms of particle number is due to neutrons and photons. The comparison shows that the higher collision energy of 10 TeV does not significantly increase the multiplicity of background particles per bunch crossing.

To quantify the origin of the BIB in a  $\sqrt{s} = 10$  TeV collider, the number of background particles as a function of the longitudinal muon decay position is reported in Fig. 2. The figure illustrates that the number of photons, electrons, positrons and neutrons drops significantly when the decay occurs outside of the final focus region. Similarly, muon decays inside the nozzle yield a negligible contribution to the BIB. The behavior is different for secondary muons (not shown in the figure), which can also reach the detector when being produced further away.

**Table 1:** Decay-induced background: number of particles entering the detector per bunch crossing (only contribution from one beam). 1.5 TeV results are from [8]. Studies assume a MAP-like nozzle.

$\sqrt{s}$	Photons	Neutrons	$e^+/e^-$	Charged hadrons	Muons
1.5 TeV	$5.0 \times 10^7$	$1.1 \times 10^8$	$8.5 \times 10^5$	$1.7 \times 10^4$	$3.1 \times 10^3$
10 TeV	$1.1 \times 10^8$	$1.0 \times 10^8$	$9.6 \times 10^5$	$4.3 \times 10^4$	$4.8 \times 10^3$



**Figure 2:** Number of background particles entering detector versus muon decay position ( $\sqrt{s} = 10$  TeV). Only one beam is simulated. The final focusing magnet positions are reported as blue rectangles for reference.

### 3. Effect of dipolar field components in the final focus region

Considering that the dominant background contribution is due to decays in the final focus region, we studied the effect of adding dipolar field components in the triplet. Inducing dispersion, a dipolar component strongly deviates the decay electrons/positrons towards the inner side of the beam chamber, until they impact on the magnet aperture. Two alternative layouts were considered, one based on combined-function dipole-quadrupoles and one based on short dipoles placed between triplet magnets. As depicted in Fig. 3, the two options give similar results. The reduction of background particles compared to a triplet without dipolar component is, however, limited.

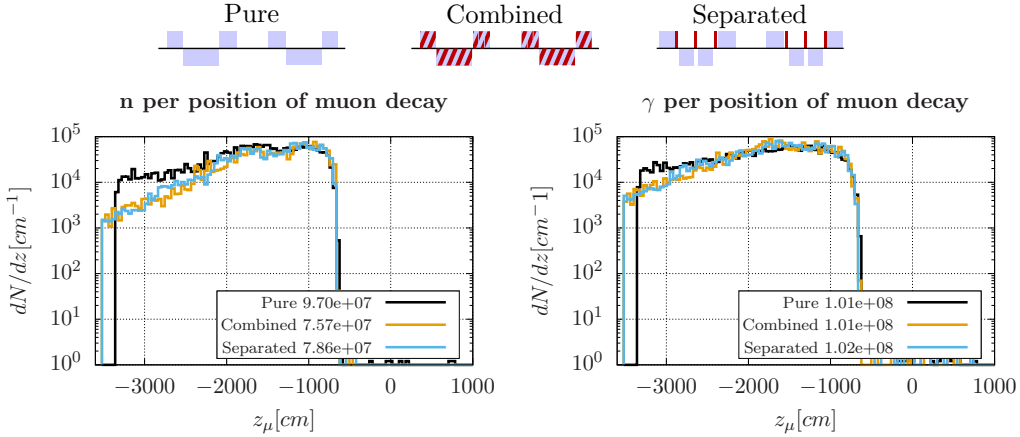


**Figure 3:** Different lattice options used in the 10 TeV collider studies. In the *pure* option, only quadrupoles are present. In the *combined* case, combined function magnets with 2 T dipolar component are considered. In the *separated* case, 1 m long dipoles (10 T) are located between triplet quadrupoles. The bottom figures show the number of background neutrons and photons per decay position.

### 4. Potential for nozzle optimization

Considering that the MAP-like nozzle in the previous sections has been optimized for the  $\sqrt{s} = 1.5$  TeV collider, the BIB suppression at higher energies can possibly still be improved. At

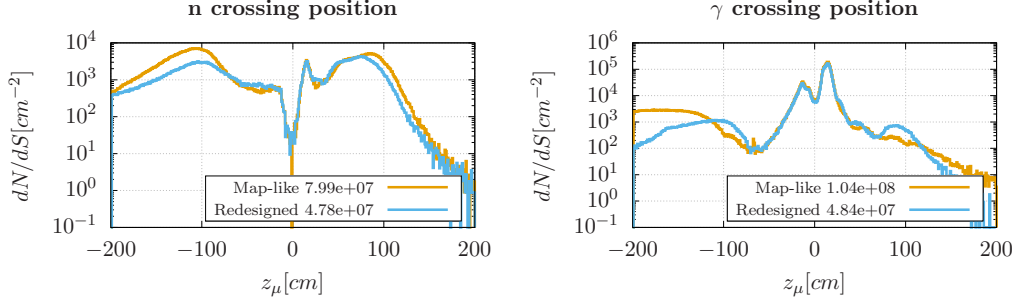


**Figure 4:** Nozzle layout effect on most abundant BIB particle species

higher energies, the decay electrons have a lower divergence and secondary cascades have a different shape. The nozzle design involves different geometrical variables, which have an influence on the BIB suppression. In this study, we attempted a first modification of the external side of the nozzle. By extending the layer of borated polyethylene and by adding an additional tungsten layer to shield photons from neutron capture, a reduction of the neutron and photon close to the IP could be achieved for the 10 TeV collider (see Fig. 4). Preliminary studies also suggest that a further reduction of the BIB can be accomplished by adjusting the nozzle tip and the inner nozzle aperture.

## 5. Other background sources

Although muon decay is the dominant source of BIB, the impact of other contributions need to be studied as well. Particularly, incoherent pair production ( $\mu^- \mu^+ \rightarrow \mu^- \mu^+ e^- e^+$ ) produces highly energetic electron/positrons pairs in the IP. In this case, the nozzle offers limited background suppression, since the particles are produced in the point where the bunch crossing occurs. To simulate this process, a list of pairs corresponding to one bunch crossing was generated using Guinea-Pig. Although the solenoid field traps a part of the produced pairs, most of the particles can still enter the detector. As shown in the energy spectrum in Fig. 5, there is a non negligible electron and positron component from pair production between 10 MeV and 1 GeV. Considering also that the particle generation is localized in vicinity of the IP, most of them will enter the inner tracker. Incoherent pair production can therefore not be neglected when studying the detector performance.

## 6. Conclusions

This paper present a first set of FLUKA Monte Carlo simulations characterizing the beam-induced background in a  $\sqrt{s} = 10$  TeV muon collider. A comparison with results previously reported in literature suggests that the background is not significantly higher than in lower energy colliders. Our studies also show that the presence of a dipolar component in the final focus region yields only a limited improvement of the background suppression, while a larger effect can be expected by optimizing the shielding configuration. We also showed that other background sources, namely incoherent pair production, cannot be neglected at  $\sqrt{s} = 10$  TeV.

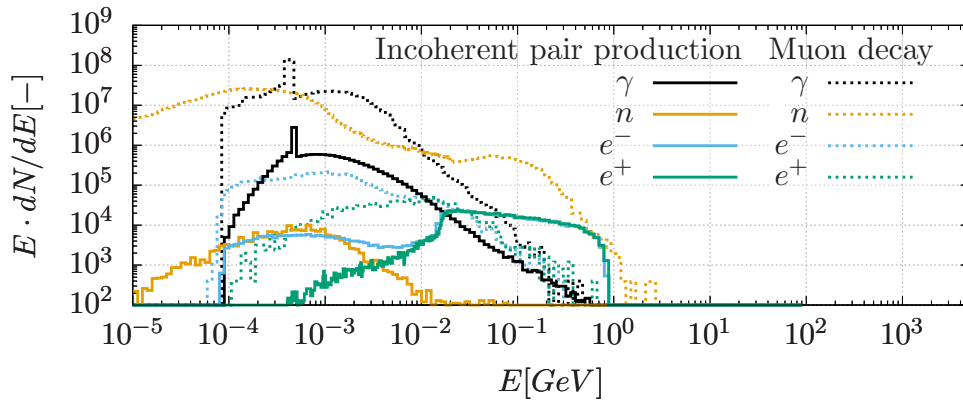


**Figure 5:** BIB energy spectrum for muon decay and incoherent pair production. Despite producing less particles, the incoherent pair production generates  $e^-/e^+$  with a significant kinetic energy.

## Acknowledgments

The authors wish to acknowledge the support from the European Union’s Horizon 2020 Research and Innovation programme under Grant Agreement No 101004730.

## References

- [1] Jean Pierre Delahaye et al. *Muon Colliders*. 2019. DOI: [10.48550/ARXIV.1901.06150](https://doi.org/10.48550/ARXIV.1901.06150).
- [2] C. Adolphsen et al. *European Strategy for Particle Physics - Accelerator R&D Roadmap*. 2022. DOI: [10.23731/CYRM-2022-001](https://doi.org/10.23731/CYRM-2022-001).
- [3] D. Schulte. *The International Muon Collider Collaboration*. 2021. DOI: [10.18429/JACoW-IPAC2021-THPAB017](https://doi.org/10.18429/JACoW-IPAC2021-THPAB017).
- [4] M. A. Palmer. *The US muon accelerator program*. 2015. DOI: [10.48550/ARXIV.1502.03454](https://doi.org/10.48550/ARXIV.1502.03454).
- [5] D. Neuffer et al. *A muon collider as a Higgs factory*. 2015. DOI: [10.48550/ARXIV.1502.02042](https://doi.org/10.48550/ARXIV.1502.02042).
- [6] N. V. Mokhov et al. *Muon Collider interaction region and machine-detector interface design*. 2012. DOI: [10.48550/ARXIV.1202.3979](https://doi.org/10.48550/ARXIV.1202.3979).
- [7] M. A. Palmer. *An Overview of the US Muon Accelerator Program*. June 2013.
- [8] F. Collamati et al. *Advanced assessment of beam-induced background at a muon collider*. Nov. 2021. DOI: [10.1088/1748-0221/16/11/p11009](https://doi.org/10.1088/1748-0221/16/11/p11009).
- [9] C. Ahdida et al. *New Capabilities of the FLUKA Multi-Purpose Code*. 2022. DOI: [10.3389/fphy.2021.788253](https://doi.org/10.3389/fphy.2021.788253).
- [10] Giuseppe Battistoni et al. *Overview of the FLUKA code*. 2015. DOI: <https://doi.org/10.1016/j.anucene.2014.11.007>.
- [11] N.V. Mokhov and S.I. Striganov. *Detector Backgrounds at Muon Colliders*. 2012. DOI: <https://doi.org/10.1016/j.phpro.2012.03.761>.